Published in final edited form as:

Traffic. 2017 July ; 18(7): 442–452. doi:10.1111/tra.12490.

Syntaxin 4 mediates endosome recycling for lytic granule exocytosis in cytotoxic T-lymphocytes

Waldo A. Spessott[1], **Maria L. Sanmillan**[1], **Vineet V. Kulkarni**[1,2], **Margaret E. McCormick**[1], and **Claudio G. Giraudo**[1,*]

[1]Department of Pathology and Laboratory Medicine, University of Pennsylvania – The Children's Hospital of Philadelphia - 3615 Civic Center Blvd, Philadelphia PA, 19104

[2]Biomedical Graduate Studies- University of Pennsylvania

Abstract

Adaptive and innate immunity utilize the perforin-killing pathway to eliminate virus-infected or cancer cells. Cytotoxic T-lymphocytes (CTLs) and Natural Killer cells mediate this process by releasing toxic proteins at the contact area with target cells known as immunological synapse (IS). Formation of a stable IS and exocytosis of toxic proteins requires persistent fusion of Rab11a recycling endosomes with the plasma membrane (PM) that may assure the delivery of key effector proteins. Despite the importance of the recycling endosomal compartment, the membrane fusion proteins that control this process at the IS remain elusive. Here, by performing knockdown experiments we found that STX4 is necessary for cytotoxic activity and CD107a degranulation against target cells in a similar fashion to STX11, which is involved in lytic granule exocytosis and immunodeficiency when it is mutated. Using TIRF microscopy we identified that STX4 mediates fusion of EGFP-Rab11a vesicles at the IS. Immunoprecipitation experiments in lysates of activated CTLs indicate that endogenous STX4 may drive this fusion step by interacting with cognate proteins: Munc18-3/SNAP23/VAMP7 and/or VAMP8. These results reveal the role of STX4 in mediating fusion of Rab11a endosomes upstream of lytic granules exocytosis and further demonstrates the importance of this pathway in controlling CTL-mediated cytotoxicity.

Graphical Abstract

[*]To whom correspondence should be addressed: giraudoc@mail.med.upenn.edu, Telephone number: 267-425-2124, Fax number: 267-426-5165.

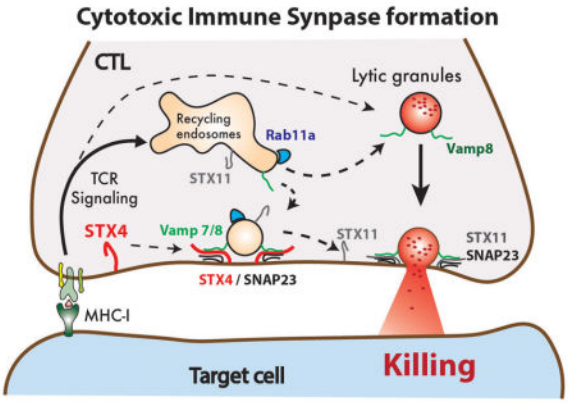

Keywords

SNARE; Syntaxin 4; Munc18-3; endosome recycling; SM protein; CTL; NK

INTRODUCTION

Cytotoxic T-lymphocytes (CTL) and Natural Killer (NK) cells play pivotal roles in host defense against viral infections and tumors[1,2]. They are responsible for killing target cells through the polarized exocytosis of cytolytic proteins such as perforin and granzymes that are contained in specialized lysosome-related organelles known as lytic granules (LGs). Recognition of foreign antigens on target cells through the T-cell receptor triggers signaling pathways that mediate the formation of a tight and well-defined structure at the interface of the two cells known as immunological synapse (IS) [3–5]. Persistent signaling at the IS induces the maturation and polarization of LGs toward the IS where they finally fuse and release they cytolytic content [6]. Previous studies have shown that continual fusion of endosomal compartments with the plasma membrane is required to sustain signaling [7–9] and to focus LG exocytosis at the IS [10,11]. However, the membrane trafficking machinery that controls these series of events are still poorly defined.

Several soluble-N-ethylmaleimide-sensitive factor attachment protein receptors (SNAREs) have been associated to the cytotoxic pathway of CTL and NK cells [6,12]. Studies in patients with defective cytotoxic activity have identified that the atypical lipid-anchored Syntaxin-11 (STX11) and its interacting Syntaxin Binding Protein 2 (STXBP2, *also known as* Munc18-2) are required for LG granule exocytosis [13–15]. Subjects harboring germline-mutations in these genes manifest with Familial Hemophagocytic Lymphohisticytosis (F-HLH-4 and F-HLH-5, respectively), a life-threatening primary immunodeficiency that results in hyper-inflammation due to an inability of the immune system to clear out viral infections or tumor cells [16]. Current evidences suggest that STX11 and Munc18-2 physically interact in multiple ways to drive the final fusion of the LG at the IS [17–20]. On the other hand, recent studies propose that VAMP8-mediated fusion of Rab11a-positive recycling endosomes (Rab11a-RE) at the immunological synapse is essential for CTL killing activity [10]. These and other studies suggest that this process might be necessary for delivering key components to the plasma membrane, such as STX11 [10] and signaling

molecules [9] that are involved in the cytotoxic immune response. Despite the importance of this membrane trafficking process, the precise SNAREs responsible for mediating fusion of Rab11a-RE at the plasma membrane are still elusive.

In this paper, we found that Syntaxin 4 (STX4) is required for cytotoxic activity of human CTLs. Although, previous studies have shown that STX4 is involved in GLUT4 transport and glucose homeostasis [21,22] as well as antibody secretion [23,24], here, we describe a novel role of STX4 in meditating membrane fusion in the secretory pathway of CTLs. We found that treatment with small interference RNAs (siRNAs) against STX4 inhibits CTL-mediated cytotoxic activity due to a reduction of LG granule fusion upon stimulation. Super-resolution microscopy imaging in fixed CTLs found that STX4 mainly localizes at the PM, as it was previously observed in other cell types [25], and partially co-localizes with anti-CD3 staining. Live cell microscopy analysis shows that STX4 is necessary for the fusion of Rab11a-RE at the IS. Additionally, co-immunoprecipitation (coIP) experiments of endogenous STX4 from human CTLs show that STX4 mainly interacts with the SM protein Munc18-3, and the SNARE proteins SNAP-23 along with either VAMP7 or VAMP8. Taken together our results indicate that STX4 is necessary for CTL-mediated cytotoxicity and suggest that the STX4/SNAP23/VAMP7 or VAMP8 SNARE complexes together with Munc18-3 are most likely responsible for the fusion or Rab11a-REs at the plasma membrane. Our data, together with previous studies, demonstrate that fusion or Rab11a-REs at the plasma membrane is an early event during the cell-killing process. Defects in this pathway may hamper downstream processes such as the cell surface delivery of critical effectors that control the cytolytic activity of CTLs and NK cells against target cells.

RESULTS

STX4 knockdown reduces cytotoxic activity of human CTLs

CTLs express several syntaxins that belong to the plasma membrane Qa-SNAREs sub-group - STX3, STX4 and STX11 [19]. Previous studies have shown that STX11 [15,18,20,26–28], but not STX3 [20] is required for CTL-mediated cytotoxicity. However, it has not been investigated yet whether STX4 is also implicated in this pathway. To test the role of STX4 in CTL-mediated cytotoxic, we silenced its expression in human CTLs using siRNAs and compared their killing activity with control CTLs treated with either non-targeting (NT), STX11 or STX3 siRNAs. Western blot analysis of whole-cell lysates of siRNA-treated cells showed that the expression level of STX4, STX11 and STX3 was reduced by approximately 70% in the corresponding knockdown cells, compared to NT-siRNA treated cells (Figure 1A and 1B). To test the specificity of the siRNA treatments, we also evaluated the expression of other syntaxins or Munc18 proteins that are necessary for secretion of cytotoxic granules [15], including Munc18-2 and Munc18-3. We did not observe a significant reduction in the expression of STX11, STX3, Munc18-2 and Munc18-3 in cells treated with different STX4 siRNAs (si-STX4-1 and si-STX4-2; Figure 1A and 1B). Similarly, STX3 and STX11-siRNA treatment did not affect the expression of other tested relevant proteins. (Figure 1A and 1B). We then tested the cytotoxic activity of these siRNA-treated cells by using a population-based re-directed cell-killing assay against anti-CD3-coated P815 target cells. Percentage of target cell lysis was measured as amount of lactate dehydrogenase (LDH) enzyme released

to the medium as described previously [17]. STX4 siRNA-treated cells exhibited over 60% reduction in target cell-killing activity compared to those treated with NT-siRNAs (Figure 1C). The reduction in cytotoxic activity of STX4 knockdown cells was comparable to the STX11 siRNA-treated cells, which were previously shown to have reduced killing activity due to impairment in lytic granule exocytosis [15,18,20,28] (Figure 1C). On the contrary, STX3 siRNA treated cells, which also exhibited almost a 70% reduction in protein expression levels (Figure 1D), showed a slight increase in cytotoxic activity compared with NT-siRNA treated cells (Figure 1C). Interestingly, knockdown of STX4 and STX11 at the same time did not have an additive effect on the cytotoxic activity. Moreover, simultaneous knockdown of STX4/STX11/STX3 did not further decrease the cytolytic activity. Taken together our results reveal that STX4, similar to STX11, is required for CTL-mediated cytotoxicity and suggest that STX4 might operate at a different step in this process.

STX4 knockdown inhibits degranulation of human CTLs

We next tested whether the reduced cytotoxic activity of cells treated with si-STX4-1 was due to an inability of LGs to fuse at the plasma membrane. To validate this, we used a flow cytometry-based “degranulation” assay that analyzes the mobilization of CD107a (a.k.a. LAMP1) from the lytic granules to the cell surface upon conjugation with anti-CD3 coated P815 target cells at 1:1 ratio [29]. Data showed that in contrast to NT and STX3 siRNA-treated cells, degranulation of STX4-1 and STX11 siRNA-treated cells was significantly reduced at the level of both percent of responding cells and induced surface CD107a expression on positive cells (Figure 2A–C). Similar degranulation defects were observed in CTLs treated with a different STX4 siRNA (si-STX4-2). Consistent with the killing assays, knockdown of STX4 and STX11 at the same time did not further decrease the degranulation activity. To evaluate the specificity of the degranulation defects in STX4 knockdown cells, we performed rescue experiments in which STX4 or NT siRNA-treated cells were transfected with either siRNA-resistant EYFP-STX4 or EYFP-STX3 constructs. Transfected cells were incubated in the absence or presence of target cells at 1:1 ratio. EYFP positive cells were analyzed for cell surface appearance of CD107a. Results showed that expression of EYFP-STX4, but not EYFP-STX3, was able to restore degranulation in STX4 knockdown cells (Figure 2D, F). In contrast, transfection of EYFP-STX4 or EYFP-STX3 in NT siRNA-treated cells did not significantly affect the degranulation activity (Figure 2E, F). Taken together, our data suggests that reduced expression of STX4 in primary human CTLs inhibits exocytosis of CD107a-containing granules and therefore their cytotoxic activity. Given that the functional phenotype of STX4-depleted cells resembles those of STX11-depleted cells, it reveals that both STX4 and STX11 are required for the cytotoxic activity of CTLs, although they might act at different steps during the exocytosis of lytic granules.

STX4 localizes at the plasma membrane of human CTLs

To better understand where STX4 works during the killing process we analyzed the subcellular localization of endogenous STX4 in both unconjugated and conjugated human CTL by using super-resolution STED microscopy. Images show that STX4 staining mainly gives a plasma membrane distribution pattern, which resembles and partially colocalizes with anti-CD3 staining, in both unconjugated and conjugated cells (Figure 3A). We also observed a small fraction of STX4 within intracellular vesicles that did not significantly

colocalize with anti-Vamp8, Rab11a or Perforin-containing vesicles as noted by the low Pearson's Colocalization Coefficient (PCC; Figure 3A–B). To examine the possibility whether STX4 knockdown reduces killing activity by affecting the size of the pool of LGs we quantified the number of perforin-containing granules in unconjugated CTLs. Results show no significant difference in the number of perforin-containing granules between STX4 and NT siRNA treated cells. These results indicate that STX4 is not involved in lytic granule biogenesis but rather argue for a role of STX4 in membrane fusion at the plasma membrane as it was described in other cell types [30–33].

STX4 is required for fusion of Rab11a compartments at the IS

We next sought to determine how reduced expression of STX4 compromises LG exocytosis at the IS. Previous studies support a model in which STX11 is responsible for the final fusion of the LGs at the IS. The failure of STX4 and STX11 to functionally compensate for each other suggests that STX4 functions at distinct steps, most likely upstream of STX11. Recent studies show that fusion of Rab11a-containing endosomes with the plasma membrane precedes LG fusion and is required for CTL-mediated cytotoxicity [10]. We, thus analyzed whether the reduced expression of STX4 in human CTLs affects the fusion of Rab11a-containing endosomes at the IS via Total Internal Reflection Fluorescent (TIRF) microscopy. To this end, we treated CTLs with either STX4, STX11 or NT siRNAs for 48 h, transiently transfected them with EGFP-Rab11a and measured fusion of EGFP-Rab11a-containing vesicles at the IS. A suspension of transfected cells was deposited onto cover glasses coated with anti-CD3, anti-CD28 and ICAM-1 to stimulate granule release. Upon contact of CTLs with the cover glass surface, the cells spread and formed a classical IS. During this time, we imaged cells by TIRF microscopy and registered the number of fusion events of EGFP-Rab11a vesicles at the plasma membrane by TIRF microscopy. A vesicle fusion event is observed by the appearance of a GFP-labeled vesicle within the TIRF plane that increases in fluorescence intensity while approaching the PM followed by a rapid radial diffusion of the fluorescent signal in the plane of the PM. (Figure 4A arrowheads, vesicle fusion#1 and #2 and Supplementary Video 1). Quantification of the number of EGFP-Rab11a vesicles fusing at the plasma membrane showed a severe reduction of fusion events in STX4 siRNA-treated CTLs compared with NT and STX11 siRNA-treated cells (Figure 4B–D and Supplementary Video 2 and 3). However, analysis of the total number of EGFP-Rab11a vesicles that appear within the TIRF plane showed no significant difference between STX4 and NT or STX11 siRNA-treated cells (Figure 4E). Since STX11 knockdown did not affect fusion of EGFP-Rab11a vesicles, it suggested that STX11 acts downstream of Rab11a vesicle fusion at the IS. Interestingly, most of the EGFP-Rab11a vesicles in STX4 siRNA-treated CTLs seemed to persist within the TIRF plane for a longer period time with a constrained lateral movement (Figure 4B, arrows and vesicle docking #1 and #2). Analysis of individual vesicles lifetime -also known as dwell-time- revealed that indeed the Rab11a-vesicle dwell-time is significantly increased in STX4 than STX11 or NT-siRNA treated cells (Figure 4F). Taken together, our results indicate that fusion, but not docking of Rab11a-containing endosomes with the PM depends on STX4 activity.

STX4 interacts with the SM protein Munc18-3 but not with Munc18-2

To identify the membrane fusion machinery that cooperates with STX4 we first tested whether SM proteins expressed in human CTLs - Munc18-2 or Munc18-3 [19]- interact with endogenous STX4. We performed a series of co-IP experiments to pull-down endogenous Munc18-2, Munc18-3 and Cathepsin S (as isotype antibody control) in lysates of primary human CTLs. In order to induce lytic granule exocytosis, and thus stimulate SNARE complex formation, CTLs were previously activated with beads coated with anti-CD3/anti-CD28 antibodies and recombinant IL-2. Bound fractions were analyzed by western blot using antibodies against STX3, STX4 and STX11 (Figure 5A and B). Interestingly, we found that Munc18-3 co-immunoprecipitated (coIPed) with STX4 but not STX11 or STX3. Conversely, Munc18-2 mainly interacts with STX11 and STX3 as it was previously reported [13,14,17,19]. We did not detect any specific association between Munc18-2 and STX4 when compared with the control IP using Cathepsin-S antibodies (Figure 5A and B). Taken together, these results strongly indicate that STX4 and STX11 associate with different SM proteins to mediate distinct membrane fusion steps during cytotoxic immune response.

Endogenous STX4 mainly interacts with SNAP23 and VAMP7/8 in primary human CTLs

To further elucidate the cognate SNAREs that contribute with STX4 for mediating Rab11a-RE fusion at the plasma membrane, we performed a series of co-IP experiments using anti-STX4, STX3, and IgG isotype control in lysates of human CTLs previously activated with CD3/CD28-coated beads. Bound fractions were analyzed by Western blot using an array of antibodies against different SNAREs proteins (Figure 6A). Results showed that endogenous SNAP23, VAMP7 and VAMP8, but not VAMP4, preferentially coIPed with STX4 when compared with STX3 and IgG IPs (Figure 6B). No VAMP2 or SNAP25 could be detected in the bound fraction either because they are not expressed in human CTLs, or they are below the detection limit as we previously described [20]. In summary, our results suggest that SNARE complexes consisting of STX4/SNAP23 and either VAMP7 or VAMP8 together with Munc18-3 might be responsible for driving Rab11a-RE fusion at the plasma for CTL-mediated killing process.

DISCUSSION

Here, we demonstrate that STX4 is required for CTL-mediated cytotoxicity. We found that silencing STX4 expression in human CTLs reduces both degranulation of CD107a vesicles and their ability to kill target cells. Although these functional defects highly resemble those of the STX11-depleted cells from patients manifesting with F-HLH-4 [15,28] and knockdown cells [18,20], we found that STX4 and STX11 mediate different membrane fusion events at the PM. While STX11 was proposed to mediate the final fusion of LGs [17,18,20,28,34,35], our data show that STX4 is necessary for fusion of Rab11a-RE at the IS prior of LG fusion. Additionally, we found that endogenous STX4 associates with a specific set of trafficking proteins consisting of Munc18-3/SNAP23 and either Vamp7 or Vamp8, most likely to drive these fusion events.

Fusion of Rab11a-RE at the immunological synapse is a critical step for normal CTL function [7,10,36]. Previous studies show that Rab11a is involved in actin remodeling and T-

cell activation [9]. Specifically, Rab11a mediates recycling of receptors and effector proteins - such as Lck or components of the T-cell receptor- to sustain signaling and thus allow the formation of a stable immunological synapse [7,36]. Additionally, it has been proposed that Rab11a recycling at the IS delivers STX11 to the PM [10,18], which is necessary for later fusion of LGs. Our results are consistent with these studies and further demonstrate that STX4 is necessary for Rab11a-RE fusion at the IS and therefore for mediating the cytotoxic immune response.

We found that endogenous STX4 localizes at the PM of human CTLs as it was previously described in other cell-types, e.g. pancreatic, adipose, epithelial, B-lymphocytes, mast cells and neurons [30–33,37]. In these cell types, STX4 mediates fusion at the plasma membrane for insulin secretion in β-cells, glucose uptake in muscle and fat cells, antibodies secretion in plasma cells and recycling of AMPA receptors in neurons. Among the known cognate SNAREs and SM proteins that cooperate with STX4 to perform these functions are SNAP23/VAMP2 or VAMP3 and Munc18-3 [30–33,38]. Similarly, we found that endogenous STX4 also interacts with SNAP23 and Munc18-3, although our data shows that STX4 associates to different vesicular SNAREs: VAMP7 and VAMP8. This is most likely because human CTLs do not express VAMP2 and have almost undetectable levels of VAMP3 [20]. Interestingly, these results are consistent with a recent report that shows that VAMP8 mediates fusion Rab11a endosomes with the PM during CTL-mediated cytotoxicity [10].

In summary, our results demonstrate that STX4 is necessary for human CTL-mediated cytoxicity against target cells by controlling early fusion events of Rab11a-RE at the IS. Our data suggest that STX4 most likely mediates these fusion events by interacting with SNAP23/VAMP7 or -8 and Munc18-3. These results may provide an explanation to the CTL cytolytic defects observed in a cohort of patients carrying heterozygous mutations in the gene encoding Munc18-3 (unpublished results from Dr. Judith Kelsen, Scott Snapper and Giraudo Labs). Although further experiments are needed to investigate the correlation of these findings, they highlight the importance of STX4-mediated fusion of Rab11a-RE for cytotoxic T-lymphocytes.

MATERIALS AND METHODS

Antibodies

Mouse anti-human STX4, -CD3, -perforin and -Lamp1 were from BD Pharmingen (San Jose, CA). Rabbit anti-VAMP7 was from Novus Biologicals (Littleton, CO). Rabbit anti-Syntaxin 11, VAMP4, VAMP8, STX3 and SNAP23 were from Synaptic System (Goettingen, Germany). Mouse anti STX11 (clone A4), Munc18-3, Munc18-2 and rabbit anti-MUNC13-4 from Santa Cruz Biotechnology (Dallas, TX). Secondary donkey anti-rabbit-800, -mouse-680 or –goat-800 were from LiCor (Lincoln, NE), goat anti-rabbit-Alexa 488 and goat anti-mouse-Alexa 546 from Invitrogen, Molecular Probes (Eugene, Oregon). CD107a-PE (clone H4A3), CD56-APC (clone NCAM16.2), CD8-FITC (clone SK1), CD3-PerCP (clone SK7) were from BD Biosciences (San Jose, CA).

Cells and Cell Lines

Written consent was obtained from healthy donors for primary $CD8^+$ T cells using a protocol approved by the Institutional Review Board at The Children's Hospital of Philadelphia. Samples were collected in EDTA tubes and processed within 24 hours of venipuncture. PBMC cells were obtained by density gradient centrifugation (Lymphoprep, Axis-Shield, Dundee, Scotland). $CD8^+$ T cells were isolated from PBMC fraction using Dynabeads untouched Human $CD8^+$ T cells kit from Invitrogen (ThermoFisher Scientific) and re-suspended in complete medium (RPMI 1640 supplemented with 10% (vol/vol) fetal bovine serum, L-glutamine, penicillin, and streptomycin; all from Invitrogen/Life Technologies, Grand Island, NY). CTLs were activated and expanded using Dynabeads (Human T-Expander CD3/CD28, Life Technologies) for 5 days in complete medium supplemented with 100 U/ml recombinant IL-2 (Proleukin-Novartis). After this time, beads were removed using a magnet and cells used for experiments. The murine P815 mastocytoma cell line was from The American Type Culture Collection (ATCC, Manassas, VA), they were cultured in complete medium (DMEM supplemented with 10% (vol/vol) fetal bovine serum, penicillin, L-glutamine and streptomycin; all from Invitrogen/Life Technologies, Grand Island, NY).

Constructs and siRNA knock-down

EGFP-Rab11a was generated by PCR amplification of the human cDNAs and subcloning into pEGFP-C1 (Clontech, Mountain View CA). $CD8^+$ T cells were transfected with the indicated plasmids using the Neon electroporator system (Thermofisher Scientific) following the manufacturer's instructions. Small-interference RNA (siRNA) knockdown experiments were performed by incubating 1.0×10^7 human CTLs with 1.0 nmol of human siGenome siRNAs (GE-Dharmacon, Lafayette- CO) followed by electroporation using Gene Pulser-II system (BioRad, Hercules CA) following manufacture's instructions. Non-Targeting (NT) siRNA consist of a pool of siRNAs catalog number D-001206-13-20 sequences: 5′-uagcgacuaaacacaucaa-3′; 5′-uaaggcuaugaagagauac-3′; 5′-auguauuggccuguauuag-3′; 5′-augaacgugaauugcucaa-3′. STX4-1 siRNA sequence 5′-cgacaggccuuaaaugaga-3′, catalog number D-016256-01. STX4-2 siRNA sequence 5′-ggacaauucggcagacuau-3′, catalog number D-016256-02. STX11 siRNA sequences 5′-ggaaggccgugcaguacga-3′, 5′-agcacugaauaucgaacaa-3′, catalog number D-019469-01 and D-019469-17, respectively. STX3 siRNA sequence 5′-gaucauugacucaacagauu-3′, catalog number D-015401-03. Cells are cultured for 48 h in complete medium and then used for different experiments. For rescue experiments we have introduced five silent nucleotide mutations (SNMs) within the sequence of human STX4 construct in order to generate a siRNA resistant construct for siSTX4-1. Underlined are the SNMs introduced in the EYFP-STX4h construct (CGACAAGCGCTGAACGAGA).

Co-immunoprecipitation assays

Primary human $CD8^+$ cells previously activated with anti-CD3, anti-CD28 coated beads and recombinant IL-2 for 4 days were lysed (25 mM Tris, 150 mM NaCl, 1 mM EDTA, 5% (vol/vol) glycerol, 1% (vol/vol) NP-40; pH 7.4) and centrifuged at 14,000 rpm for 15 min. Co-immunoprecipitation (coIP) experiments were carried out using a co-IP kit from Pierce

(Thermo Scientific). Briefly, after lysis and centrifugation, supernatants were collected and incubated with agarose beads coupled with the corresponding antibody for 20 hours at 4°C. Complexes bound to the beads were pelleted by centrifugation, followed by 5 washes with cold lysis buffer. Proteins bound to the antibodies were eluted and examined by Western blotting.

Image acquisition

CD3/CD28-activated CTLs were mixed with anti-CD3-coated P815 target cells at a 1:1 ratio, pelleted by centrifugation and incubated for 15 min to generate conjugates. Cells were then seeded in 24-well plates containing poly-lysine coated glass cover slips for 10 min at 37°C. Cells were fixed for 10 min with PBS containing 4% (vol/vol) paraformaldehyde. Cells were permeabilized with 0.1% (vol/vol) Triton X-100 in PBS buffer and then blocked with 3% (vol/vol) bovine serum albumin (BSA) in PBS for 30 min at room temperature. Immunostaining was performed using the indicated primary antibodies with secondary Atto-425 goat anti-mouse and Dylight-488 goat anti-rabbit antibodies. Cover slips were extensively washed with PBS and mounted with Prolong Gold anti-fade reagent (Thermofisher Scientific). Images were collected using a Leica SP5-STED-CW microscope (Leica Microsystems, Buffalo Grove IL). Images were analyzed using FIJI software and processed with Adobe Photoshop software.

Cytotoxicity assays

Cytotoxicity was evaluated using a non-radioactive assay (Cytotox-96, Promega, Madison, WI). To evaluate CTL killing, expanded $CD8^+$ T cells were supplemented with 10 ug/ml anti-CD3 mAb for 15 min, washed, mixed with 2×10^4 target P815 cells and incubated in quadruplicate for 4 hours at 37°C. Effector-to-target cell ratios ranged from 10 to 0.65 in 100 uL medium in 96-well V-bottom plates. After 4 hours, plates were centrifuged at 250× g for 4 min and 50 uL of supernatant were transferred to a new flat bottom 96 well plate. Fifty uL of substrate were added to each well, followed by incubation for 30 min at room temperature. The reaction was stopped using 50 uL of stop solution/well. Lactate dehydrogenase (LDH) release was measured at 490 nm using a 96 well spectrophotometer (SpectraMax, Molecular Devices, Sunnyvale, CA). Percent cytotoxicity was calculated as: Cytotoxicity (%) = (Experiment - Effector Spontaneous - Target Spontaneous/Target Maximum - Target Spontaneous) × 100.

Degranulation assay

Degranulation of CD8+ T cells was measured by incubating cells in the presence or absence of target P815 cells and anti-CD3 antibody at a 1:1 ratio for 4 h at 37°C as previously described [17,39,40]. Cells were labeled using anti-CD107a-PE, CD56-APC, CD8-FITC and CD3-PerCP. CD3+CD8+CD56− cells were gated and assessed for surface expression of CD107a. Data were acquired using an Accuri-C6 flow cytometer (BD)

TIRF Microscopy

Approximately 3.0×10^4 CTLs cells transfected with the indicated plasmids were resuspended in imaging medium RPMI–HEPES without phenol red (Thermofisher

Scientific, Waltham MA) and deposited onto a 8-well chambered coverglass (Lab-Tek II, Nunc) coated with 5ug/ml anti-CD3 (clone OKT3, BD) and anti-CD28 (BD) antibodies and 10ug/ml recombinant human ICAM-1/CD54-Fc-chimera (R&D Systems, Minneapolis MN). Cells are imaged at 10–20 frames/sec rate using a Leica DMi8 microscope equipped with ring-TIRF iLas-2 system, a dualCam with two Hamamatsu EM-CCD cameras and an environmental control system set to 5 % CO2 and 37°C. Fluorophores were excited with solid state 488 nm and 561nm lasers, TIRF angle was set to 90 nm depth. Images were analyzed and processed using FIJI software [41]. Quantification of the Rab11a vesicles dwell-time was performed using the TracMate function of FIJI software.

Supplementary Material

Refer to Web version on PubMed Central for supplementary material.

Acknowledgments

This work was supported by the PEW Charitable Trust, NIH 1R01AI123538-01A1, NIH R01GM123020, The Histiocytosis Association Award, The W.W. Smith Charitable Trust Award and the American Association for Immunologists Career Award to C.G.G.

References

1. Cerwenka A, Lanier LL. Natural killer cells, viruses and cancer. Nat Rev Immunol. 2001; 1(1):41–49. [PubMed: 11905813]
2. Orange JS, Ballas ZK. Natural killer cells in human health and disease. Clin Immunol. 2006; 118(1): 1–10. [PubMed: 16337194]
3. McCann FE, Vanherberghen B, Eleme K, et al. The size of the synaptic cleft and distinct distributions of filamentous actin, ezrin, CD43, and CD45 at activating and inhibitory human NK cell immune synapses. J Immunol. 2003; 170(6):2862–2870. [PubMed: 12626536]
4. Stinchcombe JC, Bossi G, Booth S, Griffiths GM. The immunological synapse of CTL contains a secretory domain and membrane bridges. Immunity. 2001; 15(5):751–761. [PubMed: 11728337]
5. Dustin ML, Long EO. Cytotoxic immunological synapses. Immunol Rev. 2010; 235(1):24–34. [PubMed: 20536553]
6. Luzio JP, Hackmann Y, Dieckmann NM, Griffiths GM. The biogenesis of lysosomes and lysosome-related organelles. Cold Spring Harb Perspect Biol. 2014; 6(9):a016840. [PubMed: 25183830]
7. Soares H, Henriques R, Sachse M, et al. Regulated vesicle fusion generates signaling nanoterritories that control T cell activation at the immunological synapse. J Exp Med. 2013; 210(11):2415–2433. [PubMed: 24101378]
8. Pattu V, Qu B, Marshall M, et al. Syntaxin7 is required for lytic granule release from cytotoxic T lymphocytes. Traffic. 2011; 12(7):890–901. [PubMed: 21438968]
9. Bouchet J, Del Rio-Iniguez I, Lasserre R, et al. Rac1-Rab11-FIP3 regulatory hub coordinates vesicle traffic with actin remodeling and T-cell activation. EMBO J. 2016; 35(11):1160–1174. [PubMed: 27154205]
10. Marshall MR, Pattu V, Halimani M, et al. VAMP8-dependent fusion of recycling endosomes with the plasma membrane facilitates T lymphocyte cytotoxicity. J Cell Biol. 2015; 210(1):135–151. [PubMed: 26124288]
11. Qu B, Pattu V, Junker C, et al. Docking of lytic granules at the immunological synapse in human CTL requires Vti1b-dependent pairing with CD3 endosomes. J Immunol. 2011; 186(12):6894–6904. [PubMed: 21562157]
12. de Saint Basile G, Menasche G, Fischer A. Molecular mechanisms of biogenesis and exocytosis of cytotoxic granules. Nat Rev Immunol. 2010; 10(8):568–579. [PubMed: 20634814]

13. zur Stadt U, Rohr J, Seifert W, et al. Familial hemophagocytic lymphohistiocytosis type 5 (FHL-5) is caused by mutations in Munc18–2 and impaired binding to syntaxin 11. Am J Hum Genet. 2009; 85(4):482–492. [PubMed: 19804848]
14. Cote M, Menager MM, Burgess A, et al. Munc18-2 deficiency causes familial hemophagocytic lymphohistiocytosis type 5 and impairs cytotoxic granule exocytosis in patient NK cells. J Clin Invest. 2009; 119(12):3765–3773. [PubMed: 19884660]
15. zur Stadt U, Schmidt S, Kasper B, et al. Linkage of familial hemophagocytic lymphohistiocytosis (FHL) type-4 to chromosome 6q24 and identification of mutations in syntaxin 11. Hum Mol Genet. 2005; 14(6):827–834. [PubMed: 15703195]
16. Janka GE. Familial and acquired hemophagocytic lymphohistiocytosis. Annu Rev Med. 2012; 63:233–246. [PubMed: 22248322]
17. Spessott WA, Sanmillan ML, McCormick ME, et al. Hemophagocytic lymphohistiocytosis caused by dominant-negative mutations in STXBP2 that inhibit SNARE-mediated membrane fusion. Blood. 2015; 125(10):1566–1577. [PubMed: 25564401]
18. Halimani M, Pattu V, Marshall MR, et al. Syntaxin11 serves as a t-SNARE for the fusion of lytic granules in human cytotoxic T lymphocytes. Eur J Immunol. 2014; 44(2):573–584. [PubMed: 24227526]
19. Hackmann Y, Graham SC, Ehl S, et al. Syntaxin binding mechanism and disease-causing mutations in Munc18-2. Proc Natl Acad Sci U S A. 2013; 110(47):E4482–4491. [PubMed: 24194549]
20. Spessott WA, Sanmillan ML, McCormick ME, Kulkarni VV, Giraudo CG. SM protein Munc18-2 facilitates transition of Syntaxin 11-mediated lipid mixing to complete fusion for T-lymphocyte cytotoxicity. Proc Natl Acad Sci U S A. 2017
21. Spurlin BA, Park SY, Nevins AK, Kim JK, Thurmond DC. Syntaxin 4 transgenic mice exhibit enhanced insulin-mediated glucose uptake in skeletal muscle. Diabetes. 2004; 53(9):2223–2231. [PubMed: 15331531]
22. Bryant NJ, Gould GW. SNARE proteins underpin insulin-regulated GLUT4 traffic. Traffic. 2011; 12(6):657–664. [PubMed: 21226814]
23. Rahman A, Decourcey J, Larbi NB, Loughran ST, Walls D, Loscher CE. Syntaxin-4 is essential for IgE secretion by plasma cells. Biochem Biophys Res Commun. 2013; 440(1):163–167. [PubMed: 24055037]
24. Gomez-Jaramillo L, Delgado-Perez L, Reales E, et al. Syntaxin-4 is implicated in the secretion of antibodies by human plasma cells. J Leukoc Biol. 2014; 95(2):305–312. [PubMed: 24146186]
25. Chamberlain LH, Graham ME, Kane S, et al. The synaptic vesicle protein, cysteine-string protein, is associated with the plasma membrane in 3T3-L1 adipocytes and interacts with syntaxin 4. J Cell Sci. 2001; 114(Pt 2):445–455. [PubMed: 11148145]
26. D'Orlando O, Zhao F, Kasper B, et al. Syntaxin 11 is required for NK and CD8(+) T-cell cytotoxicity and neutrophil degranulation. Eur J Immunol. 2012
27. Marsh RA, Satake N, Biroschak J, et al. STX11 mutations and clinical phenotypes of familial hemophagocytic lymphohistiocytosis in North America. Pediatr Blood Cancer. 2010; 55(1):134–140. [PubMed: 20486178]
28. Bryceson YT, Rudd E, Zheng C, et al. Defective cytotoxic lymphocyte degranulation in syntaxin-11 deficient familial hemophagocytic lymphohistiocytosis 4 (FHL4) patients. Blood. 2007; 110(6):1906–1915. [PubMed: 17525286]
29. Betts MR, Koup RA. Detection of T-cell degranulation: CD107a and b. Methods Cell Biol. 2004; 75:497–512. [PubMed: 15603439]
30. Gaisano HY, Ghai M, Malkus PN, et al. Distinct cellular locations of the syntaxin family of proteins in rat pancreatic acinar cells. Mol Biol Cell. 1996; 7(12):2019–2027. [PubMed: 8970162]
31. Rao SK, Huynh C, Proux-Gillardeaux V, Galli T, Andrews NW. Identification of SNAREs involved in synaptotagmin VII-regulated lysosomal exocytosis. J Biol Chem. 2004; 279(19):20471–20479. [PubMed: 14993220]
32. Puri N, Roche PA. Ternary SNARE complexes are enriched in lipid rafts during mast cell exocytosis. Traffic. 2006; 7(11):1482–1494. [PubMed: 16984405]

33. Jewell JL, Oh E, Thurmond DC. Exocytosis mechanisms underlying insulin release and glucose uptake: conserved roles for Munc18c and syntaxin 4. Am J Physiol Regul Integr Comp Physiol. 2010; 298(3):R517–531. [PubMed: 20053958]

34. Dieckmann NM, Hackmann Y, Arico M, Griffiths GM. Munc18-2 is required for Syntaxin 11 Localization on the Plasma Membrane in Cytotoxic T-Lymphocytes. Traffic. 2015; 16(12):1330–1341. [PubMed: 26771955]

35. Spessott WA, Sanmillan ML, McCormick ME, Kulkarni VK, Giraudo CG. SM protein Munc18-2 facilitates transition for Syntaxin 11-mediated lipid mixing to complete fusion for T-lymphocyte cytotoxicity. Proc Natl Acad Sci USA. 2017

36. Gorska MM, Liang Q, Karim Z, Alam R. Uncoordinated 119 protein controls trafficking of Lck via the Rab11 endosome and is critical for immunological synapse formation. J Immunol. 2009; 183(3):1675–1684. [PubMed: 19592652]

37. Kennedy MJ, Davison IG, Robinson CG, Ehlers MD. Syntaxin-4 defines a domain for activity-dependent exocytosis in dendritic spines. Cell. 2010; 141(3):524–535. [PubMed: 20434989]

38. Yu H, Rathore SS, Lopez JA, et al. Comparative studies of Munc18c and Munc18-1 reveal conserved and divergent mechanisms of Sec1/Munc18 proteins. Proc Natl Acad Sci U S A. 2013; 110(35):E3271–3280. [PubMed: 23918365]

39. Chiang SC, Theorell J, Entesarian M, et al. Comparison of primary human cytotoxic T-cell and natural killer cell responses reveal similar molecular requirements for lytic granule exocytosis but differences in cytokine production. Blood. 2013; 121(8):1345–1356. [PubMed: 23287865]

40. Bryceson YT, Pende D, Maul-Pavicic A, et al. A prospective evaluation of degranulation assays in the rapid diagnosis of familial hemophagocytic syndromes. Blood. 2012; 119(12):2754–2763. [PubMed: 22294731]

41. Schindelin J, Arganda-Carreras I, Frise E, et al. Fiji: an open-source platform for biological-image analysis. Nat Methods. 2012; 9(7):676–682. [PubMed: 22743772]

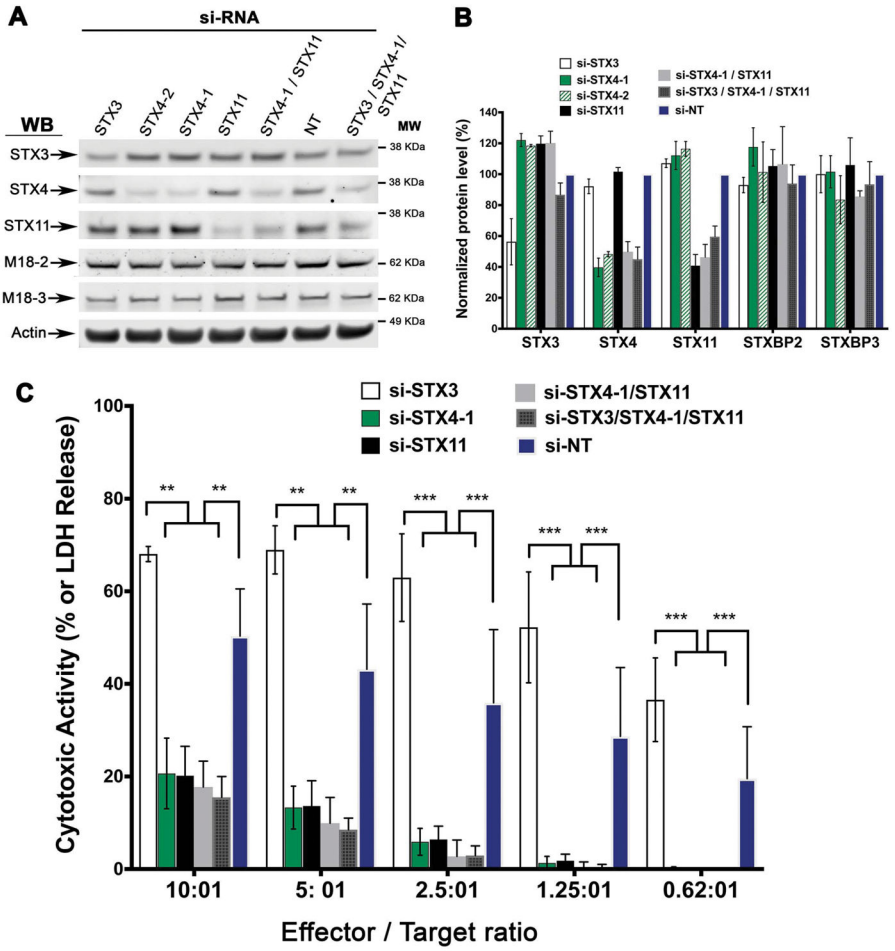

Figure 1. STX4 knockdown affects killing activity of normal control CTLs

(**A**) Human CTLs were electroporated with two different STX4 siRNAs (STX4-1, STX4-2) or with either non-targeting (NT), STX11 or STX3 siRNAs or a combination of them STX4/STX11, STX4/STX11/STX3 and cultured for 48 h. Cell lysates were analyzed by W.B. for the indicated proteins. **(B)** Quantification of knockdown efficiency in W.B. shown in A. Blots are representative of four independent experiments. (**C**) Cytotoxicity assay to measure CTL-mediated cell killing. Equivalent numbers of CTLs (effectors) from each condition were incubated with anti-CD3 antibody in the presence or absence of P815 target cells (targets) at the indicated cell ratios. The killing assay was run for 4 h at 37°C and the amount of LDH released into the supernatant was quantified using a Cytotox-96 assay. Data are the mean ± SEM of four independent experiments run in quadruplicates. ** *p<0.01; ***p<0.001*

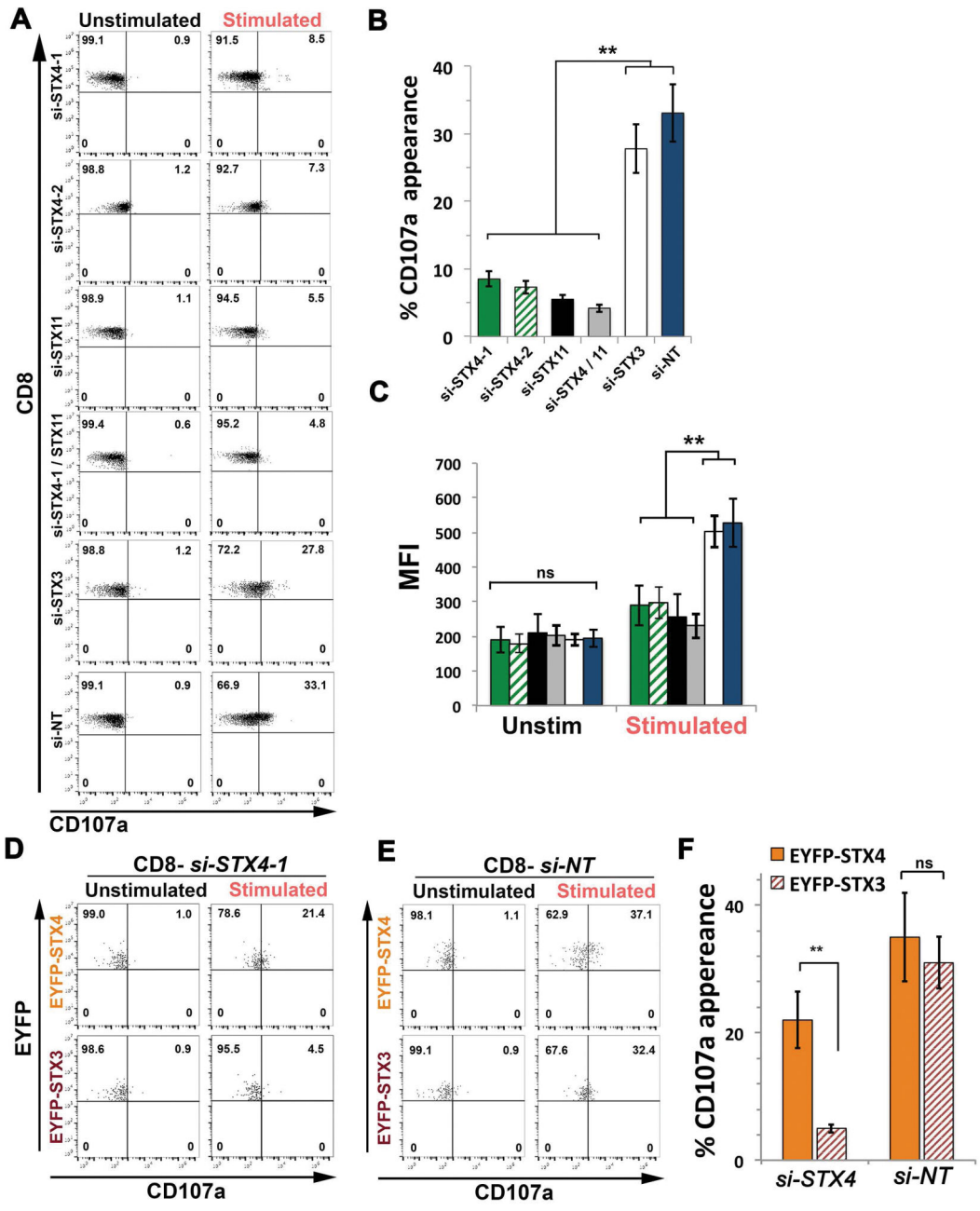

Figure 2. STX4 knockdown affects CD107a degranulation activity of normal control CTLs

(**A**) Human CTLs treated with siRNAs against either STX4-1, STX4-2, STX11, STX3, NT, or with both STX4 and STX11 used in Figure 1, were assessed for CD107a degranulation upon activation with target cells using Effector/Target cell ratio 1/1. Briefly, siRNA-treated CTLs were incubated for 4 h at 37°C in the presence or absence of P815 cells previously treated with anti-CD3 antibody. Cells were stained using anti-CD107a-PE, anti-CD56-APC, anti-CD8-FITC and anti-CD3-PerCP antibodies and analyzed by flow cytometry. $CD3^{+}CD8^{+}CD56^{-}$ cells were gated and analyzed for the appearance of CD107a on the surface upon incubation with target cells. Plots are representative of 4 independent

experiments. (**B**) Graphs showing the percentage of cells that increased CD107a staining upon stimulation. (**C**) Mean fluorescence intensity (MFI) values in the CD107a-PE channel of unstimulated (Unstim) versus stimulated (Stim) cells. Results are the mean ± SD of four independent measurements. ** $p<0.01$. (**D**) Expression of a siRNA resistant EYFP-STX4 construct, but not of EYFP-STX3, restored CD107a degranulation in STX4 knockdown CTLs. Plots are representative of two independent experiments. (**E**) Expression of either a siRNA resistant EYFP-STX4 or EYFP-STX3 do not further increased CD107a degranulation in control CTLs treated with NT siRNAs. Plots are representative of two independent experiments. (**F**) Graphs showing the percentage of cells that increased CD107a staining upon stimulation in rescue experiments shown in D and E. Results are the mean ± SD of two independent measurements. ** $p<0.01$.

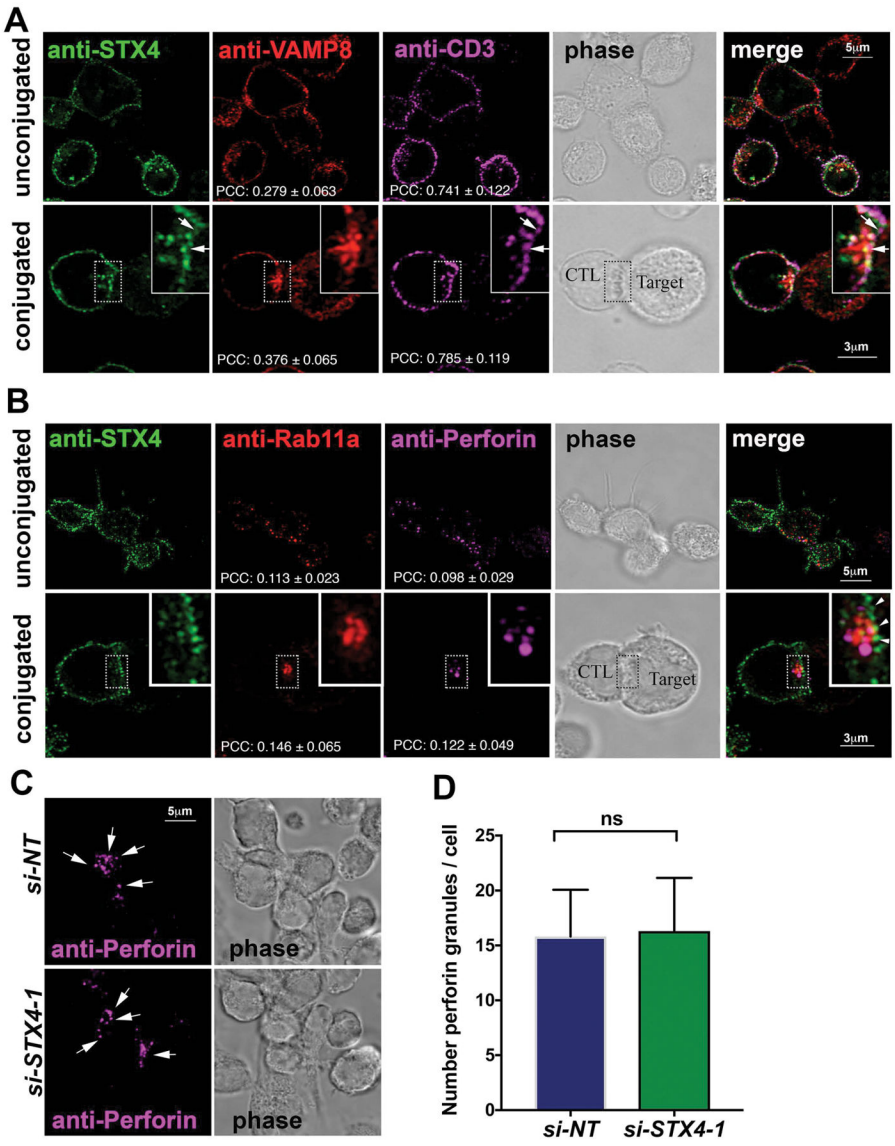

Figure 3. STX4 localizes at the PM of human CTLs

(**A**) STX4 partially colocalizes with CD3 at the PM. CTLs from normal control individuals were incubated for 20 min in the absence (unconjugated) or presence (conjugated) of anti-CD3 and P815 cells at a 1:1 ratio for 15 min at 37°C and seeded onto poly-lysine coated coverslips. Cells were fixed, permeabilized and stained using anti-STX4, anti-Vamp8 and followed by anti-CD3-Alexa 647 staining. Arrows show areas of colocalization between STX4 and CD3. Inserts display a zoomed in view of the selected area. Pearson's colocalization coefficient (PCC) was determined for STX4/VAMP8 and STX4/CD3. Data are mean ± SD; n=15 cells. Bar equals 5 μm in unconjugated cells and 3 μm in conjugated cells. (**B**) STX4 does not co-localize with Perforin or Rab11a. CTLs from normal control individuals were immune stained as explained in A, but using anti-STX4, anti- Rab11a and followed by anti-Perforin-Alexa 647 staining. Arrowheads show areas where STX4 is at IS and RAB11A and perforin containing vesicles make close contact. Inserts display a zoomed

in view of the selected area. Pearson's co-localization coefficient (PCC) was determined for STX4/Rab11a and STX4/Perforin. Data are mean ± SD; n=15 cells. Bar equals 5 μm in unconjugated cells and 3 μm in conjugated cells. (**C**) STX4 knockdown does not affect the number of perforin-containing granules. Normal control CTLs treated with either STX4-1 or NT siRNAs were subjected to immunofluorescence using anti-perforin antibody. Arrows point to perforin granules. **D**) Quantification of the perforin containing granules per cell does not show any statistical significant difference between STX4-1 and NT siRNA-treated cells. Data are the mean ± SEM; n=35 cells.

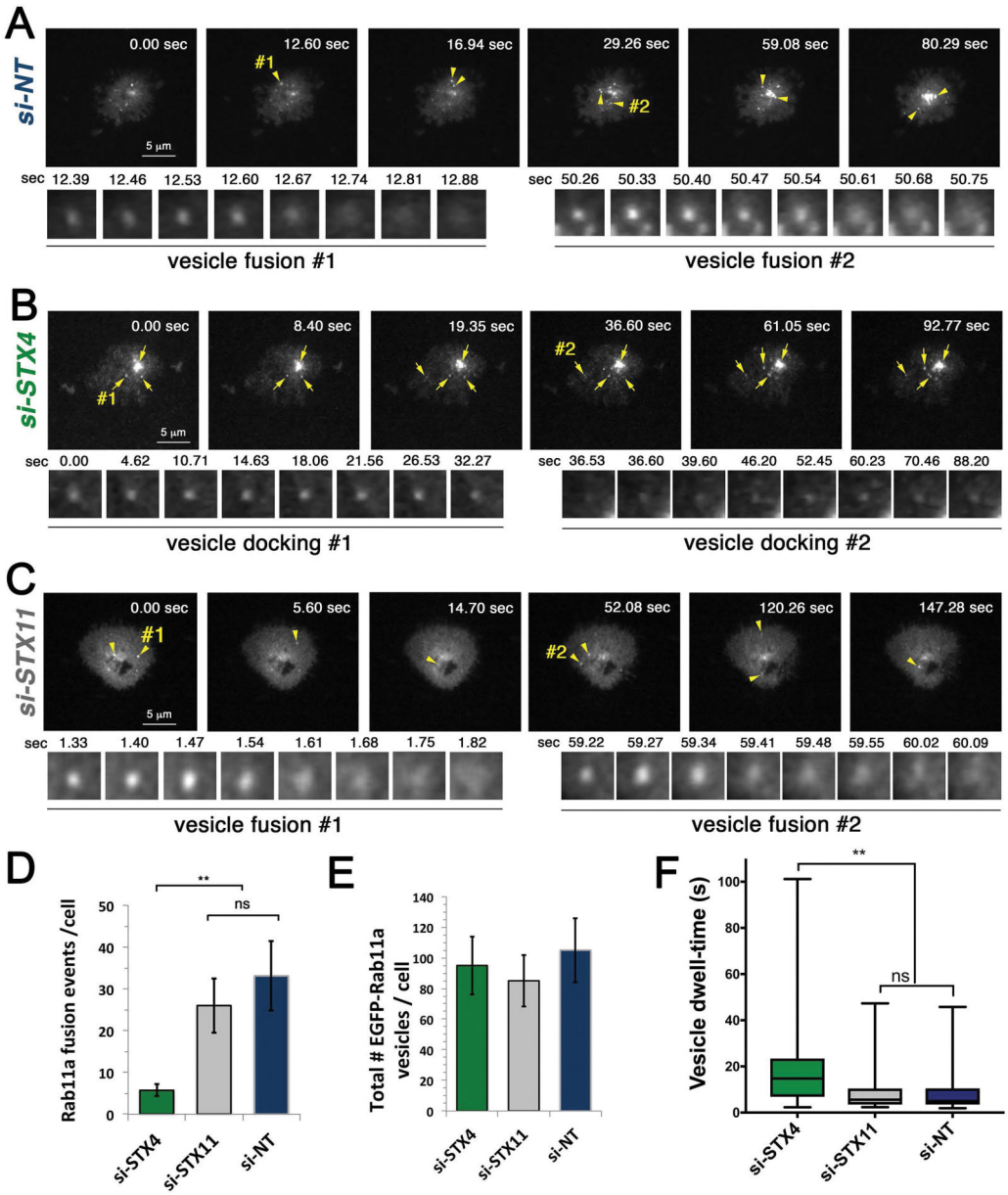

Figure 4. STX4 mediates fusion of EGFP-*Rab11a* vesicles at IS

Human CTLs treated with either NT, STX4-1 or STX11 siRNAs were transfected with a EGFP-Rab11a construct, incubated for 24 h and deposit onto poly-lysine treated coverslips coated with activation molecules anti-CD3 and anti-CD28 antibodies and ICAM1 for live cell TRIF imaging. Upon contacting the surface, CTLs spread and form a classical immunological synapse. During this time we imaged cells by TIRF microscopy at about 14 frame per second interval and the number of fusion events of EGFP-Rab11a vesicles at the plasma membrane were registered. Images show representative cells with the sequence of events in NT siRNA treated cells (**A**), STX4 (**B**) or STX11 siRNA-treated cells **(C)**. Arrowheads point to vesicles that arrived to the TIRF plane producing an increase in fluorescent intensity and subsequently fuse with the plasma membrane exhibiting a lateral

diffusion of the GFP-construct on the plasma membrane within a few frames. Two representative fusion events are shown in **A** and **C -** vesicle fusion #1 and #2. Relative time of the movie is shown on the upper right corner in seconds. Arrows point to vesicles that arrived to the evanescent TIRF plane and remain there without fusing with the plasma membrane. Two representative events are shown in **B** -vesicle docking #1 and #2. (**D**) Plot showing the quantification of number of EGFP-Rab11a fusion events at the plasma membrane per cell. Data are mean ± SEM. n=10 cells. (**E**) Plot showing the quantification of the total number of EGFP-Rab11a that entered within the TIRF plane per cell during 3 min of imaging. Data are mean ± SEM. n=10 cells. **F**) Plot showing the quantification of the time that each EGFP-Rab11a vesicles persisted within the TIRF plane, i.e. dwell-time. Data are mean ± SEM. n = 250 vesicles from 4 different cells. ** $p<0.01$.

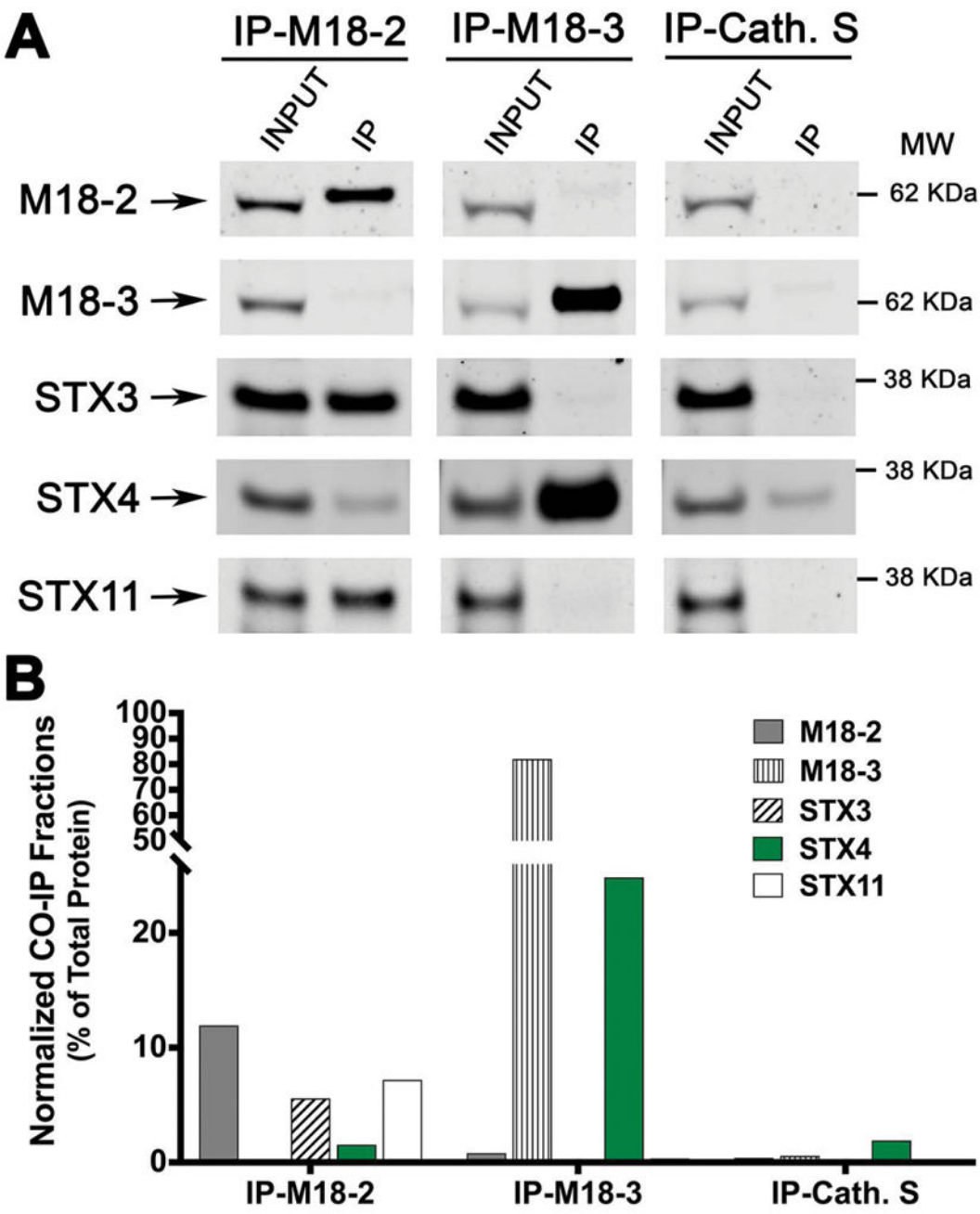

Figure 5. STX4 associates with Munc18-3 but not with Munc18-2 in human CTLs

(**A**) Co-immunoprecipitation experiments of the SM proteins: Munc18-2 and Munc18-3 using lysates generated from healthy control CTLs activated with anti-CD3/anti-CD28 coated beads. Endogenous Munc18-2 or Munc18-3 were immunoprecipitated using goat anti–Munc18-2, anti-Munc18-3 or anti-Cathepsin-S (Cath. S, as isotype control) antibodies and the amount of different CTL relevant Syntaxins; STX3, STX4 and STX11 that co-immunoprecipitated was analyzed by Western blotting. (**B**) Bands in the Western blot that corresponded to the fraction of STXs that co-precipitated with either Munc18-2, Munc18-3 or Cath. S were quantified by densitometry and normalized to the total amount of each

protein present on the cell lysate used for the IPs. Results are representative of three independent experiments.

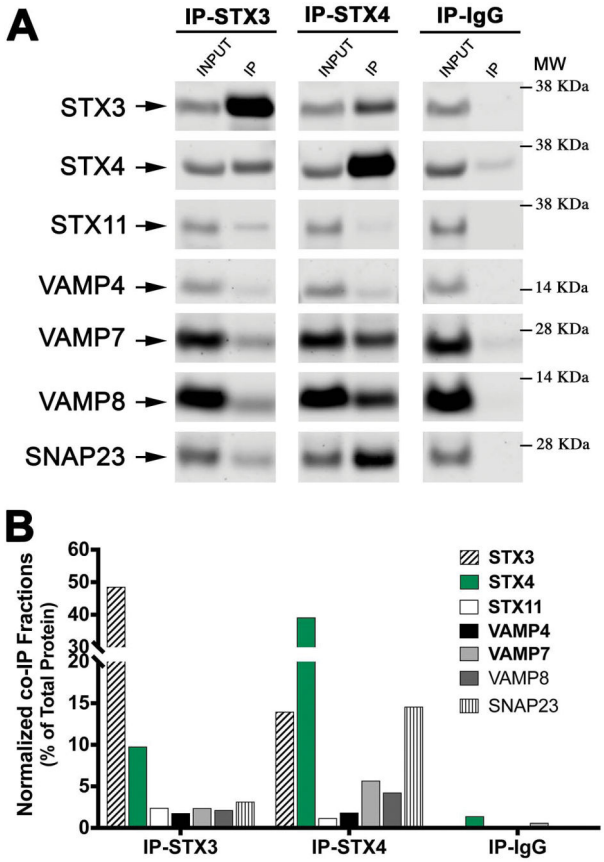

Figure 6. STX4 associates with SNAP23 and either VAMP7 or VAMP8 in human CTLs

(**A**) Co-immunoprecipitation experiments using rabbit anti–STX3, anti-STX4, or IgG isotype control antibodies were performed in lysates generated from healthy control CTLs activated with anti-CD3/anti-CD28 coated beads. The amount of different CTL relevant endogenous SNAREs: STX3, -4, -11, VAMP4, -7, -8 and SNAP23 that co-immunoprecipitated was analyzed by Western blotting. (**B**) Bands in the Western blot that corresponded to the fraction of SNAREs that co-precipitated with either STX3, STX4 or IgG control were quantified by densitometry and normalized to the total amount of each protein present on the cell lysate used for the IPs. Results are representative of three independent experiments.